# MICROCHONDRULES; RECORDS OF MULTIPLE HEATING EVENTS IN THE SOLAR NEBULA AND IMPLICATIONS FOR TYPE II CHONDRULE FORMATION.

J. N. Bigolski[1,2,3], M. K. Weisberg[1,2,3], D. S. Ebel[2,3], H. C. Connolly Jr. [1,2,3,4], [1]Dept. Phys. Sci., Kingsborough Community College CUNY, Brooklyn, NY 11235, USA (jbigol@gmail.com), [2]Earth and Envi. Sci., CUNY Graduate Center, New York, NY 10016, USA, [3]Dept. Earth and Planet. Sci., American Museum of Natural History, New York, NY 10024, USA, [4]Lunar and Planetary Laboratory (LPL), Univ. of Arizona, Tucson, AZ 85721, USA.

**Introduction:** Three of the most primitive unequilibrated ordinary chondrites (UOCs) have two distinct populations of chondrules; their characteristic chondrules (~ 1mm apparent dia.) and microchondrules (apparent diameters ≤ 40µm). Microchondrules have been previously described in UOCs [e.g. 1–3] and in CR chondrite matrix and dark inclusions [4]. FeO-rich, dusty silicate rims surround 65% of chondrules in UOCs [5]. A ubiquitous component of these rims, microchondrules are found within ~20% of the rims around MgO-rich, FeO-poor (Type I) chondrules; microchondrules are absent from rims surrounding MgO-poor, FeO-rich (Type II) chondrules [5, 6].

We previously reported on microchondrules in UOCs [6] and have increased our database with new bulk chemical data on microchondrules and chondrules. We use our data to test the following hypotheses that microchondrules are products of localized heating within dusty microenvironments that persisted at close proximity to chondrules during the latter's acquisition of dusty rims either: (1) due to multiple heating events in dusty nebular regions by a mechanism such as gas shock waves or current sheets, or (2) via a single-stage impact on the planetesimal-scale.

**Analytical Techniques:** A total of 48 microchondrules were analyzed in thin-sections of Northwest Africa 5717 (NWA 5717-1; Ung.3.05), Bishunpur AMNH 532-2 (LL3.15), and Semarkona AMNH 4128-5 (LL3.00) using a JSM-6390 LV/LGS scanning electron microscope (SEM) with a Quantax 200 Energy Dispersive X-ray spectrometer at Kingsborough Community College and the Hitachi S4700 field emission SEM and Cameca SX100 electron microprobe at the AMNH. Microprobe operating conditions were an accelerating voltage of 15 kV, a beam current of 20 nA, and a dwell time of 20 s for all elements (Mg, Al, Si, Ca, Cr, Mn, Fe) with the exception of Na, which had a 10 s dwell time. Microchondrules were analyzed using a 1 µm point beam. Owing to their small grain size and cryptocrystalline and glassy textures, each microchondrule analysis represents a bulk composition. Bulk analyses of 30 chondrules from NWA 5717, Semarkona and Watonga (Watonga-2; LL3.10) were obtained using a 25 µm spot.

**Results:** *Texture:* Microchondrules occur in two textural setting in UOCs: as inclusions within fine-grained chondrule rims and less commonly (~7%) as inclusions within Fe-sulfide and Fe-Ni-metal rich clasts in the matrix. Similarly to chondrules, they have textures that include cryptocrystalline (C), microporphyritic (MP), radial pyroxene (RP) and glassy (Fig. 1). The "rim microchondrules" analyzed are embedded components of fine-grained rims that surround Type I chondrules (Fig. 1a-c); no microchondrules are found within the rims of Type II chondrules. The "matrix microchondrules" are all glassy. Some microchondrules (Fig. 1d) have numerous vesicles.

*Bulk Composition (all in wt. % oxide):* Microchondrules have similar average bulk compositions, except for the glassy ones which are more silica-rich (Table 1). C-microchondrules (n=29) are mostly magnesian with CaO<1.0 %, yet some are more calcic and moderately FeO-rich (1.0-4.2 CaO, 3.1-12.0 FeO). The average bulk compositions in Table 1 do not reflect the FeO-enriched microchondrules shown in Fig. 1a. These have 18.0-46.8 FeO with fayalite-normative compositions. MP-microchondrules (0.6-9.4 CaO, 2.3-12.4

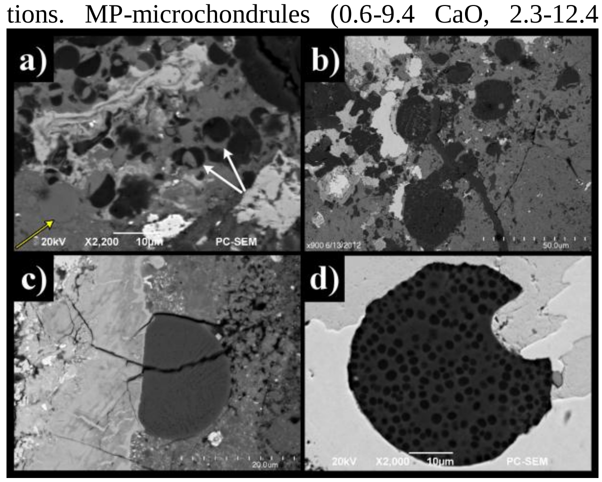


Fig. 1. Backscattered electron images showing microchondrule textural types. a) C-microchondrules and round mineral fragments in a fine-grained rim. Some micros show partial (right arrows) or complete FeO enrichment (yellow arrow). b) and c) MP- and RP-textures, respectively. d) Glassy microchondrule from the matrix that has numerous 0.5-2.0 µm vesicles.

Table 1. Average bulk compositions of microchondrules (wt. % oxide). Sampling size in parantheses.

| Texture | $Na_2O$ | MgO | $Al_2O_3$ | $SiO_2$ | CaO | $Cr_2O_3$ | MnO | FeO |
|---|---|---|---|---|---|---|---|---|
| **C (29)** | 0.5 | 32.6 | 0.9 | 52.8 | 1.4 | 0.9 | 0.6 | 9.4 |
| **MP (8)** | 0.8 | 30.0 | 1.9 | 54.5 | 3.2 | 0.9 | 0.6 | 7.7 |
| **RP (6)** | 0.3 | 33.6 | 1.3 | 56.7 | 1.4 | 0.7 | 0.3 | 4.7 |
| **Glassy (5)** | 2.9 | 6.3 | 15.4 | 61.6 | 7.9 | 0.7 | 0.4 | 3.5 |

FeO; n=8) and RP-microchondrules (0.8-3.4 CaO, 1.6-7.3 FeO; n=6) compositionally overlap the range of C-microchondrules. Glassy microchondrules (n=5) are Si- and Al-rich (64.6-68.1 $SiO_2$, 7.0-19.2 $Al_2O_3$) with 3.6-15. CaO. Other glassy microchondrules are albite-normative (4.9 $Na_2O$, <1.0 CaO). In general, microchondrules have a range of bulk compositions that overlap those of the chondrules (Fig. 2), with ~50% of the C-microchondrules and all RP-microchondrules with Mg# vs. Mn and Cr relationships similar to Type I chondrules (Fig. 2). Less common (~31%) are C-microchondrules with Mg#'s that overlap or are below those of Type II chondrules. Such C-microchondrules are FeO-enriched (e.g., Fig. 1a).

**Discussion & Implications:** The predominance of nonporphyritic textures among the microchondrules in UOCs (~80%), as well as their primary location within chondrule rims, suggests that these spherules formed as rapidly cooled droplets within close proximity to the chondrules. The relatively small size of microchondrules implies rapid dissipation of heat; C- and glassy microchondrules would have experienced faster cooling rates (>500ºC/hr) than those of MP- and RP-textures [e.g., 7]. The presence of MP- and RP-textures

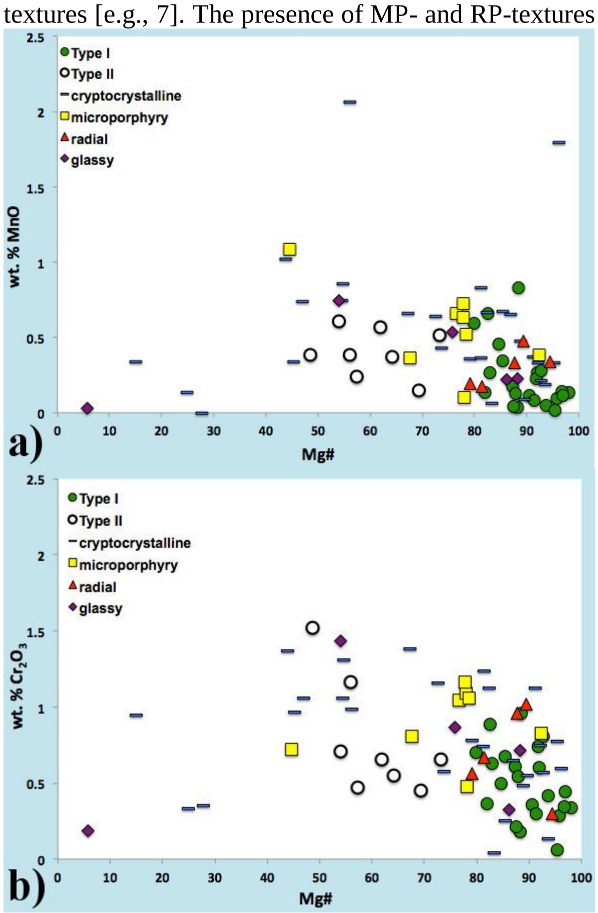


Fig. 2. Bulk composition of microchondrules and Type I/Type II chondrules. Mg# = 100×Mg/(Mg+Fe) wt. %.

suggests that melt droplets acquired dust before final crystallization of microchondrules [8].

The large compositional overlap between microchondrules and chondrules (Fig. 2) suggests a genetic relationship, although the lack of microchondrules in Type II chondrule rims implies that Type II chondrules formed in a spatially or temporally distinct environment or through a different process than Type I chondrules. We propose that Type I chondrules and/or their precursors acquired FeO-rich silicate dust either during or shortly after exposure to flash heating events in the nebula. A similar heating mechanism must have also produced the two distinct size populations of chondrules in UOCs: mm-sized chondrules (down to ~0.1 mm) as well as the microchondrules (≤ 40 µm). We interpret this as evidence for multiple heating events during a time when Type I chondrules were actively acquiring dusty rims. The The accretion of forsteritic olivine and/or enstatite with ice [e.g., 9] and Fe-metal grains could result in the oxidation of metal and FeO-enrichment of magnesian silicates. The remelting of these accretionary assemblages (Type I chondrules and their FeO-rich rims) could produce Type II chondrules with relict magnesian phenocrysts and is consistent with Type I olivine relicts in Type II chondrules [9].

We hypothesize a four-stage process: 1) Formation of Type I chondrules due to shock waves or current sheets; 2) Type I chondrules pass through dusty regions and acquire coatings of fine-grained minerals and ice; 3) Heating of dusty chondrule assemblages results in microchondrule formation and oxidation of Fe. 4) Some of the original Type I chondrules are heated to the point of remelting host chondrule and ferroan dusty coatings to produce FeO-rich melt and Type II chondrules as an end product. Many Type I chondrules, however, experienced less intense heating, thus producing irregular chondrule shapes, as well as microchondrules embedded in sintered, fine-grained FeO-rich silicate rims. The abundance of microchondrules within different chondrite groups may record the intensity of heating events and/or recycling of chondrule materials. This does not, however, preclude potentially deleterious effects of aqueous alteration.

**References:** [1] Rubin A. E. et al. (1982) GCA, *46*, 1763-1776. [2] Krot A. N. and Rubin A. E. (1996) In *Chondrules and the Protoplanetary Disk* (R. H. Hewins et al., eds.), 181-184, Cambridge UP. [3] Krot A. N. et al. (1997) GCA, *61*, 463-473. [4] Weisberg M. K. et al. (1993) GCA, *57*, 1567-1586. [5] Bigolski J. N. et al. (2013) *XLIV*, Abstract #2239. [6] Bigolski J. N. et al. (2012) *XLIII*, Abstract #2426. [7] Desch S. J. and Connolly Jr., H. C. (2002) MAPS, *37*, 183-207. [8] Connolly Jr., H. C. and Hewins R. H. (1995) GCA, *59*, 3231-3246. [9] Connolly Jr., H. C. and Huss G. R. (2010) GCA, *74*, 2473-2483.